Available online at www.sciencedirect.com

SciVerse ScienceDirect

Ceramics International 39 (2013) 6099–6106

CERAMICS INTERNATIONAL

www.elsevier.com/locate/ceramint

Predicting Charpy impact energy of Al6061/SiC_p laminated nanocomposites in crack divider and crack arrester forms

Hesam Pouraliakbar[a,c], Ali Nazari[b,*], Pouriya Fataei[b], Akbar Karimi Livary[a], Mohammad Jandaghi[c]

[a]Department of Advanced Materials, WorldTech Scientific Research Center (WT-SRC), Tehran, Iran
[b]Department of Modeling and Simulation, WorldTech Scientific Research Center (WT-SRC), Tehran, Iran
[c]Department of Materials Science and Engineering, Sharif University of Technology, Azadi Ave., Tehran, Iran

Received 17 December 2012; received in revised form 9 January 2013; accepted 9 January 2013
Available online 1 February 2013

Abstract

Charpy impact energy of the produced Al6061–SiC_p laminated nanocomposites by mechanical alloying was modeled by adaptive neuro-fuzzy interfacial systems (ANFIS) in both crack divider and crack arrester configurations. The model was constructed by training, validating and testing of 171 gathered input–target data. The thickness of layers, the number of layers, the adhesive type, the crack tip configuration and the content of SiC nanoparticles were five independent input parameters utilized for modeling. The output parameter was Charpy impact energy of the nanocomposites. The performance of the proposed models was evaluated by absolute fraction of variance, the absolute percentage error and the root mean square error and the best values of 0.9945, 3.521 and 8.224, respectively acquired for them. The results introduced ANFIS as an influential tool for predicting the Charpy impact energy of the considered Al6061–SiC_p laminate nanocomposites.

Keywords: A. Extrusion; Metal–matrix composites; Impact behavior; Modeling

1. Introduction

Metal–matrix nanocomposites on the basis of aluminum and such hard reinforcements as nano-SiC have been widely considered in the recent scientific research on account of their appropriate properties which normally could not be present in many engineering structures. The main efforts have been conducted on providing such matrix that contains uniformly dispersed hard reinforcements. The produced homogenous structure will result in distinguished properties which make these materials useful even for aerospace science [1,2]. Among the proposed method to attain such uniform structure is high-energy mechanical milling and subsequent canning into suitable container to protect the produced nanocomposite powder from the possible environmental reaction. Afterwards, the densified powder is extruded to achieve the highest possible density and mechanical properties [2,3].

Al–SiC (nano)composites have been produced successfully by several researchers. Hanada et al. [4] Al–30 vol%-SiC composites showed excellent compressive properties such as yield stress, ultimate strength, and fracture strain. Those were produced by fine SiC particulates incorporated into an aluminum matrix by mechanical alloying. Structural and morphological aspects of Al–5 vol%SiC nanocomposite powder produced by mechanical alloying were considered by Khadem et al. [5] as a reasonable matrix. The results revealed the average particle size < 10 nm and coefficient of variation < 0.1 achievement by the increased milling time up to more than 10 h. Again mechanical alloying was employed by Hanada et al. [6] to disperse fine SiC particulates in an aluminum–lithium matrix powder. A homogenous distribution of reinforcements had accquired finer grain structure (< 1 μm) to the aluminum–lithium nanocomposite as they claimed. El-Eskandarani [7], Woo and Zhang [8] and Lu et al. [9] were among the other researchers who studied

*Corresponding author. Tel.: +98 912 2208049.
E-mail address: anazari@worldtech-src.com (A. Nazari).

0272-8842/$ - see front matter © 2013 Elsevier Ltd and Techna Group S.r.l. All rights reserved.
http://dx.doi.org/10.1016/j.ceramint.2013.01.027

production of Al–SiC (nano)powders and evaluated the subsequent (nano)composite.

As stated in Ref. [10], Al/SiC_p nanocomposites may possess low impact resistance. Appropriate methods should be considered to improve this property. The proposed method in the previous work was lamination of the bulk composites into several layers which results in plane-stress with the increased impact resistance. The only two works on investigating Charpy impact energy of Al–nano SiC laminated composites is related to those done in Refs. [10,11].

Adaptive network-based fuzzy inference systems (ANFIS) a famous hybrid neuro-fuzzy network for modeling the complex systems [12] was successfully adopted for predicting Charpy impact resistance of Al/epoxy laminated composites in both crack arrester and crack divider configurations [13]. As an incorporator of the human-like reasoning style of fuzzy systems through the use of fuzzy sets and a linguistic model consisting of a set of IF–THEN fuzzy rules, ANFIS models are universal approximators [12] with the ability to solicit interpretable IF–THEN rules. Nowadays, ANFIS, an artificial intelligence-based technique, have been successfully applied in the engineering applications in spite of the lack of using this program in metallurgical aspects of engineering materials. Especially this is very limited in the field of Al–SiC nanocomposites. Even other common techniques such as artificial neural networks (ANNs) are rarely developed for prediction of the properties of these materials. Rather than the works done in Refs. [10,11], the only related work is that of Dashtbayazi et al. [14] who only modeled the synthesizing parameters of Al–8 vol%SiC nanocomposites by ANNs and not the properties of the produced material.

In this work, Charpy impact energy of Al/SiC_p nanocomposites in both crack divider and crack arrester configurations have been modeled by ANFIS. A total number of 171 pair input–target data were collected from Refs. [10,11], trained, validated and tested by the constructed networks. The performance of the constructed models was examined by characteristics data accuired by training, testing and validating data. The proposed models show their capability for prediction of Charpy impact energy of Al6061–SiCp laminated nanocomposites in both crack divider and crack arrester forms in the considered range.

2. Data collection

The data were collected from Refs. [10,11]. The method of production Al6061–SiCp laminated nanocomposites and production Charpy impact test for the subsequent standard examinations was in the following order:

At first, Al6061 powder with the average particles size of 75 μm produced by nitrogen gas atomization and SiC nanoparticles with the particle sizes less than 100 nm were ball-milled for 45 min. After that, aluminum cans with the internal diameter of 60 mm, the external diameter of 62 and the height of 110 mm were stored in a steel mold, filled by the produced powder in several layers and finally the powder were cold-pressed under a pressure of 220 MPa. The cans were pre-heated in an argon atmosphere at 490 °C for 1 h and then the compressed powders were extruded under a drag pressure of 1750 MPa and a velocity of 2.5 mm/s with a ratio of 16:1 to produce slabs with a surface area of 250×15 mm^2.

Two-, five- and ten-layer laminated specimens, along with the monolithic specimen were produced to consider the influence of laminate architecture on the impact resistance. A 10 mm thick Al6061/SiC_p bar was used to make the monolithic specimen while the layers thicknesses in two-, five- and ten-layer laminated specimens were 5, 2 and 1 mm, respectively. The thickness of the specimen was 10 mm in accordance to the standard size of Charpy specimens which was determined by ASTM E23 standard [15]. Therefore, the number of layers in two-, five- and ten-layer laminated specimens was 5, 2 and 1 mm, respectively.

The adhesive materials were selected from the previous work [13]. A two-part epoxy polymer, including resin and curing agent which were modified by using core–shell rubber particles, a methacrylated butadiene-styrene (MBS) copolymer with a nominal diameter of less than 380 nm, and silicon carbide particles (SiC). The average particle size of the utilized SiC particles was 15 μm. The additive contents (both SiC and MBS) were 5 vol% in accordance to Ref. [13] in which the highest strength was achieved.

Charpy impact specimens were notched perpendicular to the interface of the layers using a diamond saw in both crack divider and crack arrester configurations with the notches' depth of 2 mm. The impact energy of the produced laminated nanocomposites was evaluated using Charpy impact specimens according to the ASTM E23 [15].

3. Architecture of ANFIS used in this study

The architecture of an ANFIS model with two input variables and two fuzzy IF–THEN rules of Takagi and Sugeno's type could be stated as follows:

- Rule 1: IF x is A_1 and y is B_1, THEN $f_1 = p_1x + q_1y + r_1$.
- Rule 2: IF x is A_2 and y is B_2, THEN $f_2 = p_2x + q_2y + r_2$.

The basic learning rule of ANFIS, the back-propagation gradient descent, calculates error signals recursively from the output layer backward to the input nodes and is exactly the same as the back-propagation learning rule used in the common feed-forward neural networks [16,17]. As indicated in Refs. [13,16,17], recently, ANFIS adopted a rapid learning method named as hybrid-learning method which utilizes the gradient descent and the least-squares method to find a practicable set of predecessor and resultant parameters [16,17] and therefore is used in this study as adopted in Ref. [13].

The structure of the two proposed ANFIS networks in the present study was consisted of five independent input variables incorporating the thickness of layers (T), the number of layers (N), the adhesive type (A), the crack tip configuration (C) and the content of SiC nanoparticles (S). The output parameter was Charpy impact energy of the laminated nanocomposites (CVN) in both crack divider and crack arrester configurations. The input space was decomposed by three fuzzy labels. In this paper, such as the previous one [13], two types of membership functions (MFs) including the triangular (ANFIS-I) and Gaussian (ANFIS-II) were utilized to construct the suggested models and comparing their capability. From the total 171 experimental data, the proposed ANFIS models were trained by 121 haphazardly selected input–target pairs, validated by other 25 randomly chosen and tested by the remaining 25 pair of data. Furthermore, to guarantee the gaining of the minimum error tolerance, up to 1000 epochs were specified for training process.

Matlab ANFIS toolbox was used for ANFIS programming and to overcome optimization difficulty, a program was developed in Matlab which handles the trial and error process—automatically [18–21]. The program endeavors various selected functions and when the highest RMSE (Root Mean Squared Error) of the testing set, as the training set, is achieved, it was reported [18–21].

The IF–THEN rules in the present work were achieved by supposing that the rule base of ANFIS contains different fuzzy IF–THEN rules of Takagi and Sugeno's type [12,22]:

- Rule 1: IF T is A_i, N is B_i, A is C_i, C is D_i and S is E_i THEN $f_i = p_iT + q_iN + r_iA + s_iC + t_iS + u_i$.
- Rule 2: IF T is A_j, N is B_j, A is C_j, C is D_j and S is E_j THEN $f_j = p_jT + q_jN + r_jA + s_jC + t_jS + u_j$.

The corresponding equivalent ANFIS architecture is shown in Fig. 1 and the functions of each layer could be represented as follows:

Layer 1—Every node i or j in this layer is a square node with a node function:

$$O_i^1 = \mu_{A_i}(T) \quad i = 1, 2 \tag{1}$$

$$O_i^1 = \mu_{B_i}(N) \quad i = 1, 2 \tag{2}$$

$$O_i^1 = \mu_{C_i}(A) \quad i = 1, 2 \tag{3}$$

$$O_i^1 = \mu_{D_i}(C) \quad i = 1, 2 \tag{4}$$

$$O_i^1 = \mu_{E_i}(S) \quad i = 1, 2 \tag{5}$$

where T, N, A, C and S are inputs to node i, and A_i, B_i, C_i, D_i and E_i are the linguistic label (fuzzy sets: small, large, …) associated with this node function.

Layer 2—Every node in this layer is a circle node labeled Π which multiplies the received signals and sends the product out. For example,

$$W_i = \mu_{A_i}(T) \times \mu_{B_i}(N) \times \mu_{C_i}(A) \times \mu_{D_i}(C) \times \mu_{E_i}(S), \quad i = 1, 2 \tag{6}$$

Each node output illustrates the firing weight of a rule.

Layer 3—Every node in this layer is a circle node labeled as N and the ith node computes the ratio of the ith rule's firing weight to the sum of all rule's firing weights:

$$W_i = W_i/(W_1/W_2), \quad i = 1, 2 \tag{7}$$

Layer 4—Every node in this layer is a square node with a node function:

$$O_i^4 = \overline{w}_i(P_iT + q_iN + r_iA + s_iC + t_iS + u_i) \tag{8}$$

where $\overline{w}_i$ is the output of layer 3, and $\{p_i, q_i, r_i, s_i, t_i, u_i\}$ is the parameter set.

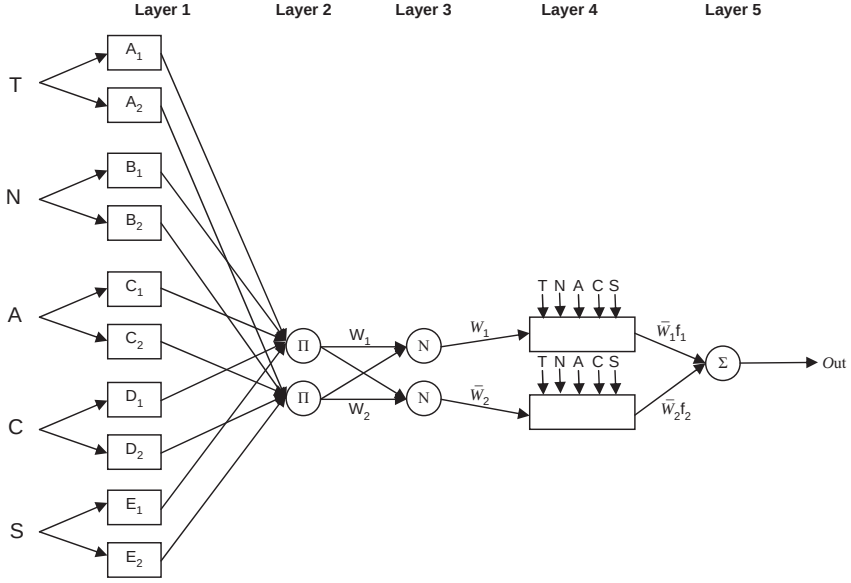

Fig. 1. Schematic of ANFIS architecture utilized in this work.

Layer 5—The signal node in this layer is a circle node labeled R that computes the overall output as the summation of all incoming signals, i.e.,

$$O_i^5 = \sum_i \overline{w}_i f_i = \sum_i w_i f_i / \sum_i w_i \quad (9)$$

4. Predicted results and discussion

The performance of the constructed networks in the present study during the training, validating and testing in ANFIS-I and ANFIS-II models was examined in terms of absolute fraction of variance (R^2), the absolute percentage error (MAPE) and the root mean square error (RMSE) which are calculated by Eqs. (10)–(12), respectively [23]:

$$R^2 = 1 - \left(\frac{\sum_i (t_i - o_i)^2}{\sum_i (o_i)^2} \right) \quad (10)$$

$$MAPE = \frac{1}{n} \sum_i \left| \frac{t_i - o_i}{t_i} \right| \times 100 \quad (11)$$

$$RMSE = \sqrt{\frac{1}{n} \sum_i (t_i - o_i)^2} \quad (12)$$

where t is the target value, o is the output value and n is the number of data sets in each of training, validating and testing phases.

The entire collected data and those predicted by using the training, validating and testing results of both ANFIS-I and ANFIS-II models are given in Fig. 2a, b and c, respectively. The linear least square fit line, its equation and R^2, MAPE and RMSE values have been shown in these figures for the training, validating and testing data. In addition, inputs values and collected data with validating and testing results obtained from ANFIS-I and ANFIS-II models have been given in Tables 1–4. Fig. 2 shows a very close relationship between the collected experimental data and those acquired from the training, validating and testing in ANFIS-I and ANFIS-II models. Fig. 2c for the testing sets show the capability of ANFIS-I and ANFIS-II models for generalizing between input and output variables with an appropriate manner.

The performance of both ANFIS-I and ANFIS-II models is shown in Fig. 2. The maximum value of R^2 and the minimum values of MAPE and RMSE are 0.9945, 3.521 and 8.224, respectively, all in training phase of ANFIS-II model. The minimum value of R^2 and the maximum ones of MAPE and RMSE are 0.9709, 6.021 and 14.22, respectively in testing sets of ANFIS-II, ANFIS-I and ANFIS-I models, in that order. The entire R^2, MAPE and RMSE values show that the proposed ANFIS-I and ANFIS-II models are appropriate approaches and can predict the Charpy impact energy of Al6061–SiCp laminated nanocomposites very close to the collected experimental values [13].

In the Ref. [10], Charpy impact energy of Al6061–SiCp laminated nanocomposites was predicted by ANNs and in

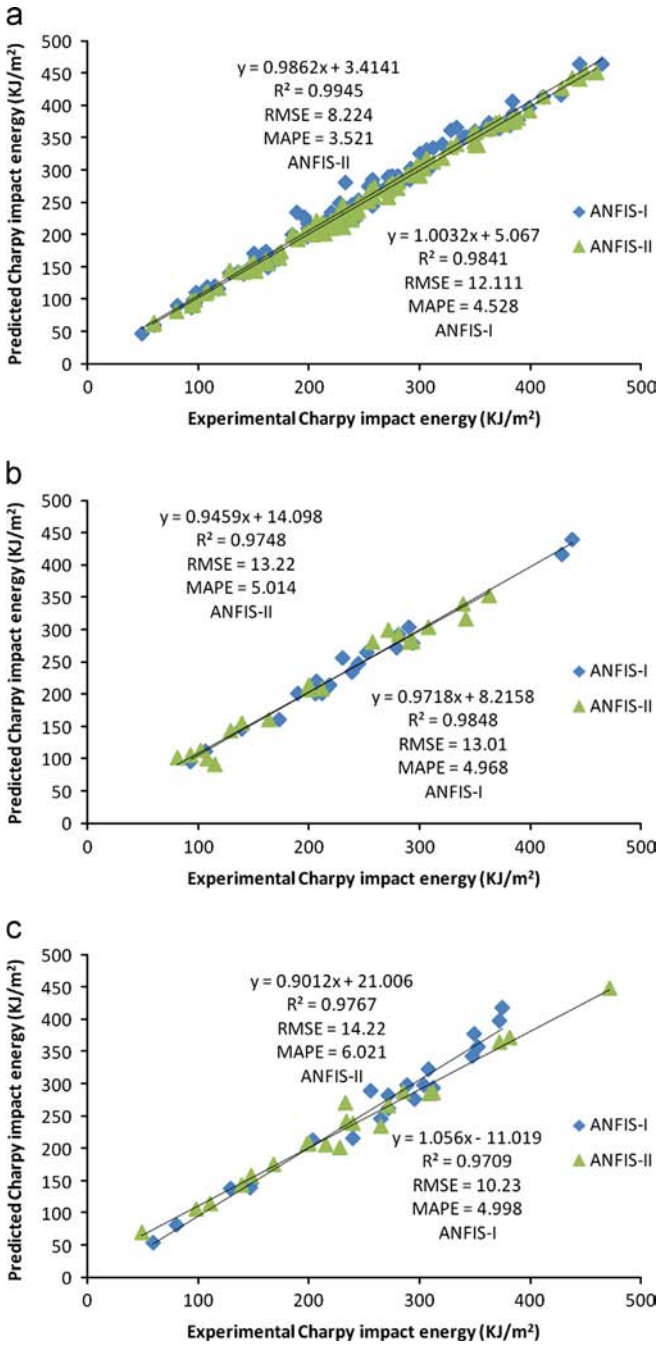

Fig. 2. The correlation of the collected data and predicted Charpy impact energy values of Al6061–SiC_p laminated nanocomposites in (a) training, (b) validation and (c) testing phase for ANFIS models.

Ref. [11] it was predicted by gene expression programming (GEP).

In Ref. [10], two models were conducted by ANNs and the performance of the network was only evaluated by means of R^2 values. The performance of those models was near to those predicted in the present study where the maximum and minimum values of R^2 were 0.9958 and 0.9672, respectively. This shows the accuracy of the both ANN and ANFIS models. However, the superiority of the presented work is considering the performance of the models by three characteristic assessments as R^2, RMSE

Table 1
Data sets for comparison of the gathered experimental data with results predicted from the ANFIS-I model in validation phase.

Predicted CVN (KJ/m^2)	Experimental CVN (KJ/m^2)	SiC content (vol%)	Crack tip configuration[b]	Adhesive type[a]	Number of layers	Thickness of layer (mm)	Sample number
101.3	81	2	1	0	1	10	6
90.96	115	3	1	0	1	10	12
160.2	164	2	2	1	2	5	20
213.5	200	2	2	1	5	2	26
207.27	199	2	2	3	5	2	37
208.39	212	3	2	1	2	5	51
280.42	257	3	2	2	5	2	58
316	342	3	2	2	10	1	62
339.12	339	3	2	3	10	1	66
99.9	108	5	2	1	2	5	68
105.87	93	5	2	2	2	5	70
113.03	102	5	2	3	2	5	78
155.38	139	5	2	2	5	2	81
143.45	129	5	2	3	5	2	105
302.99	308	2	3	2	5	2	108
284.12	292	2	3	3	5	2	110
352.73	363	2	3	1	10	1	120
298.89	272	3	3	1	2	5	121
282.64	294	3	3	2	2	5	122
292.34	281	3	3	2	2	5	125
280.65	291	3	3	3	2	5	138
421.22	428	3	3	1	10	1	141
455.3	465	3	3	2	10	1	152
164.62	169	5	3	3	2	5	155
193.65	210	5	3	1	5	2	6

[a]0, 1, 2 and 3 are respectively for monolithic nanocomposite, neat epoxy, M5 and S5 adhesives.
[b]1, 2 and 3 are respectively for monolithic nanocomposite, crack divider configuration and crack arrester configuration.

Table 2
Data sets for comparison of the gathered experimental data with results predicted from the ANFIS-I model in testing phase.

Predicted CVN (KJ/m^2)	Experimental CVN (KJ/m^2)	SiC content (vol%)	Crack tip configuration[b]	Adhesive type[a]	Number of layers	Thickness of layer (mm)	Sample number
70.04	49	5	1	0	1	10	7
158.31	148	2	2	1	2	5	11
207.2	200	2	2	3	5	2	25
270.86	233	2	2	3	10	1	36
207.32	198	3	2	1	2	5	38
205.89	215	3	2	2	2	5	42
106.28	98	5	2	2	2	5	69
113.69	111	5	2	3	2	5	71
143.52	139	5	2	3	5	2	79
201.4	228	5	2	2	10	1	87
241.92	234	2	3	2	2	5	94
238.75	240	2	3	3	2	5	97
233.91	265	2	3	3	2	5	99
266.56	272	2	3	1	5	2	100
287.42	285	2	3	1	5	2	101
286.46	312	2	3	2	5	2	103
284.29	309	2	3	3	5	2	107
363.87	372	3	3	2	5	2	130
372.27	381	3	3	3	5	2	134
448.4	472	3	3	3	10	1	143
174.94	168	5	3	1	2	5	145
169.1	158	5	3	1	2	5	147
155.02	151	5	3	3	2	5	151
266.64	253	5	3	2	10	1	166
279.87	286	5	3	3	10	1	170

[a]0, 1, 2 and 3 are respectively for monolithic nanocomposite, neat epoxy, M5 and S5 adhesives.
[b]1, 2 and 3 are respectively for monolithic nanocomposite, crack divider configuration and crack arrester configuration.

Table 3
Data sets for comparison of the gathered experimental data with results predicted from the ANFIS-II model in validation phase.

Predicted CVN (KJ/m^2)	Experimental CVN (KJ/m^2)	SiC content (vol%)	Crack tip configuration[b]	Adhesive type[a]	Number of layers	Thickness of layer (mm)	Sample number
112	106	3	1	0	1	10	5
160	173	2	2	2	2	5	15
214	219	2	2	2	5	2	22
220	207	2	2	2	5	2	24
247	245	2	2	1	10	1	28
264	252	2	2	3	10	1	34
202	212	3	2	1	2	5	37
209	215	3	2	2	2	5	42
234	239	3	2	3	2	5	44
271	279	3	2	1	5	2	47
96	93	5	2	2	2	5	68
148	139	5	2	2	5	2	78
146	139	5	2	3	5	2	79
201	190	5	2	1	10	1	82
201	206	5	2	2	10	1	85
255	230	2	3	2	2	5	95
304	290	2	3	3	5	2	106
280	294	3	3	2	2	5	121
292	281	3	3	2	2	5	122
416	429	3	3	1	10	1	137
439	438	3	3	2	10	1	139
450	450	3	3	2	10	1	140
450	460	3	3	3	10	1	142
173	160	5	3	3	2	5	153
211	210	5	3	1	5	2	155

[a]0, 1, 2 and 3 are respectively for monolithic nanocomposite, neat epoxy, M5 and S5 adhesives.
[b]1, 2 and 3 are respectively for monolithic nanocomposite, crack divider configuration and crack arrester configuration.

Table 4
Data sets for comparison of the gathered experimental data with results predicted from the ANFIS-II model in testing phase.

Predicted CVN (KJ/m^2)	Experimental CVN (KJ/m^2)	SiC content (vol%)	Crack tip configuration[b]	Adhesive type[a]	Number of layers	Thickness of layer (mm)	Sample number
81	80	2	1	0	1	10	3
54	59	5	1	0	1	10	8
139	147	2	2	2	2	5	13
146	148	2	2	2	2	5	14
262	272	2	2	1	10	1	30
282	272	2	2	2	10	1	32
289	256	3	2	3	5	2	52
357	353	3	2	2	10	1	59
138	129	5	2	3	5	2	81
213	203	5	2	3	10	1	88
216	240	2	3	3	2	5	97
246	265	2	3	3	2	5	99
293	312	2	3	2	5	2	103
297	289	2	3	2	5	2	104
322	308	2	3	2	5	2	105
377	349	2	3	1	10	1	111
397	372	2	3	3	10	1	116
418	375	2	3	3	10	1	117
277	295	3	3	1	2	5	118
298	304	3	3	2	2	5	123
343	348	3	3	1	5	2	127
465	472	3	3	3	10	1	143
165	175	5	3	1	2	5	146
191	206	5	3	2	5	2	159
193	190	5	3	3	5	2	161

[a]0, 1, 2 and 3 are respectively for monolithic nanocomposite, neat epoxy, M5 and S5 adhesives.
[b]1, 2 and 3 are respectively for monolithic nanocomposite, crack divider configuration and crack arrester configuration.

and MAPE. As one may know, the performance of the model could not be only predicted by R^2 values since the slope of the line correlating experimental and predicting data may be greater or smaller than 1 while their relationship remains constant. Other evaluators such as MAPE and RMSE are required to show this better. However, since Ref. [10] shows the experimental work as well, it could be considered as a suitable work.

In Ref. [11], 4 models based on GEP were proposed to predict the Charpy impact energy of Al6061–SiCp laminated nanocomposites. The superiority of that work was the presented equations that relate the Charpy impact energy to the input parameters. In addition, the performance of the models was considered by R^2, RMSE and MAPE. The maximum value of R^2 and the minimum values of MAPE and RMSE were 0.9811, 10.317 and 12.613, respectively. The minimum value of R^2 and the maximum ones of MAPE and RMSE were 0.9696, 13.110 and 15.429, respectively. A comparison between these results and those obtained in the present study illustrate the capability of ANFIS model to present more accurate results. However, a direct equation in GEP model could depict its powerful nature. However, the time of training is much more in GEP models than that of ANNs and ANFIS models.

One of the superiority of the present work is eliminating test trial number which in Refs. [10,11] was considered as the 6th input variable. The predicted results by ANFIS here show that this factor has no effect on the performance of the proposed models and one may predict the Charpy impact energy of Al6061–SiCp laminated nanocomposites by the five proposed independent input parameters.

On the whole, one may consider each of ANNs, GEP or ANFIS as a suitable artificial intelligent technique for predicting the Charpy impact energy of the considered Al6061–SiCp laminated nanocomposites.

5. Conclusions

In the present study, two different ANFIS models were proposed for predicting the Charpy impact energy of Al6061–SiCp laminated nanocomposites in both crack divider and crack arrester forms. The difference between the ANFIS models was in their considered Triangular (ANFIS-I) and Gaussian (ANFIS-II) membership functions. ANFIS model constructed by Gaussian membership function revealed better performance characteristics especially in training phase. However, both models illustrated a high accuracy for predicting the Charpy impact energy. The performance of the constructed models was evaluated by R^2, RMSE and MAPE where the maximum value of R^2 and the minimum values of MAPE and RMSE achieved are 0.9945, 3.521 and 8.224, respectively, all in training phase of ANFIS-II model. On the other hand, the minimum value of R^2 and the maximum ones of MAPE and RMSE are 0.9709, 6.021 and 14.22, respectively in testing sets of ANFIS-II, ANFIS-I and ANFIS-I models, in that order. The performance of the proposed models was compared by those of the previous work and it was concluded that artificial intelligence techniques, incorporating ANFIS, are appropriate tools for approaching the Charpy impact energy of the considered laminated nanocomposites.

References

[1] S.C. Tjong, Novel nanoparticle-reinforced metal matrix composites with enhanced mechanical properties, Advanced Engineering Materials 9 (8) (2007) 639–652.

[2] S. Kamrani, A. Simchi, R. Riedel, S.M. Seyed Reihani, Effect of reinforce- ment volume fraction on mechanical alloying of Al–SiC nanocomposite, Powder Metallurgy 50 (2007) 276–282.

[3] R. Rahmani Fard, F. Akhlaghi, Effect of extrusion temperature on the microstructure and porosity of A356–SiC_p composites, Journal of Materials Processing Technology 187–188 (2007) 433–436.

[4] K. Hanada, K.A. Khor, M.J. Tan, Y. Murakoshi, H. Negishi, T. Sano, Aluminium–lithium/SiCp composites produced by mechanically milled powders, Journal of Materials Processing Technology 67 (1997) 8–12.

[5] S.J. Hong, P.W. Kao, SiC-reinforced aluminium composite made by resistance sintering of mechanically alloyed powders, Materials Science and Engineering A 119 (1989) 153–159.

[6] S.A. Khadem, S. Nategh, H. Yoozbashizadeh, Structural and morphological evaluation of Al–5 vol%SiC nanocomposite powder produced by mechanical milling, Journal of Alloys and Compounds 509 (2011) 2221–2226.

[7] M.S. EL-Eskandarani, Mechanical solid state mixing for synthesizing of SiCp/Al nanocomposites, Journal of Alloys and Compounds 279 (1998) 263–271.

[8] K.D. Woo, D.L. Zhang, Fabrication of Al–7 wt%Si–0.4 wt%Mg/SiC nanocomposite powders and bulk nanocomposites by high energy ball milling and powder metallurgy, Current Applied Physics 4 (2004) 175–178.

[9] L. Lu, M.O. Lai, C.W. Ng, Enhanced mechanical properties of an Al based metal matrix composite prepared using mechanical alloying, Materials Science and Engineering A 252 (2003) 203–211.

[10] A. Nazari, V. Abdinejad, Artificial neural networks for prediction Charpy impact energy of Al6061/SiCp laminated nanocomposites, Neural computing and Applications (2012)http://dx.doi.org/10.1007/s00521-012-0996-0.

[11] A. Nazari, V. Abdinejad, Modeling Charpy impact behavior of Al6061/SiCp laminated nanocomposites by genetic programming, Ceramics International 39 (2) (2013) 1991–2002.

[12] JSR Jang, ANFIS: adaptive-network-based fuzzy inference system, IEEE Transactions on Systems, Man, and Cybernetics 23 (3) (1993) 665–685.

[13] A. Nazari, A. Sedghi, N. Didehvar, Modeling impact resistance of aluminum–epoxy-laminated composites by artificial neural networks, Journal of Composite Materials 46 (13) (2012) 1593–1605.

[14] M.R. Dashtbayazi, A. Shokuhfar, A. Simchi, Artificial neural network modeling of mechanical alloying process for synthesizing of metal matrix nanocomposite powders, Materials Science and Engineering A 466 (2007) 274–283.

[15] ASTM E23, Standard test methods noteched bar impact testing of me6tallic materials, ANFISual book of ASTM standards, ASTM, Philadelphia, PA, 2001.

[16] I.B. Topcu, M. Sarıdemir, Prediction of mechanical properties of recycled aggregate concretes containing silica fume using artificial neural networks and fuzzy logic, Computational Materials Science 42 (1) (2008) 74–82.

[17] J.S.R. Jang, C.T. Sun, Nuro-fuzzy modeling and control, Proceedings of IEEE 83 (3) (1995).

[18] I.H. Guzelbey, A. Cevik, A. Erklig, Prediction of web crippling strength of cold-formed steel sheetings using neural networks, Journal of Constructional Steel Research 62 (2006) 962–973.

[19] I.H. Guzelbey, A. Cevik, M.T. Gögüs, Prediction of rotation capacity of wide flange beams using neural networks, Journal of Constructional Steel Research 62 (2006) 950–961.
[20] A. Cevik, I.H. Guzelbey, Neural network modeling of strength enhancement for Cfrp confined concrete cylinders, Building & Environment 43 (2008) 751–763.
[21] A. Cevik, I.H. Guzelbey, A Soft, Computing based approach for the prediction of ultimate strength of metal plates in compression, Engineering Structures 29 (3) (2007) 383–394.
[22] A.A. Ramezanianpour, M. Sobhani, J. Sobhani, Application of network based neuro-fuzzy system for prediction of the strength of high strength concrete, Amirkabir Journal of Science and Technology 5 (59-C) (2004) 78–93.
[23] I.B. Topcu, M. Sarıdemir, Prediction of compressive strength of concrete containing fly ash using artificial neural network and fuzzy logic, Computational Materials Science 41 (3) (2008) 305–311.